

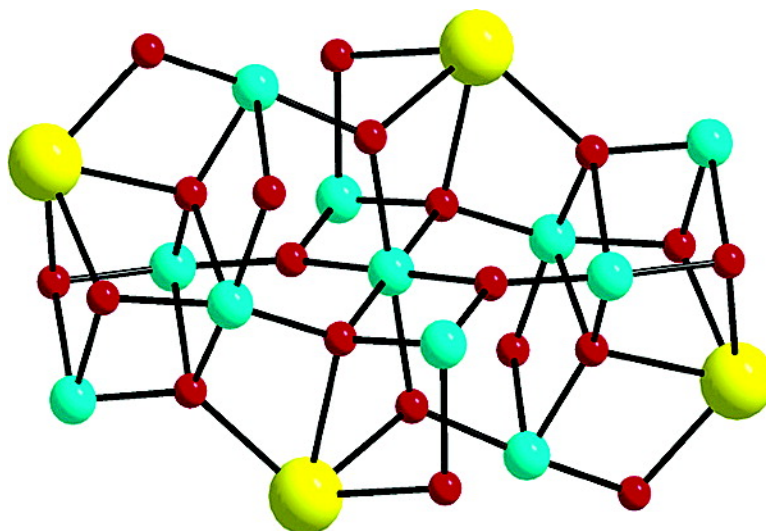
Communication

## Initial Observation of Magnetization Hysteresis and Quantum Tunneling in Mixed Manganese–Lanthanide Single-Molecule Magnets

Abhudaya Mishra, Wolfgang Wernsdorfer, Khalil A. Abboud, and George Christou

*J. Am. Chem. Soc.*, **2004**, 126 (48), 15648-15649 • DOI: 10.1021/ja0452727 • Publication Date (Web): 12 November 2004

Downloaded from <http://pubs.acs.org> on April 5, 2009



### More About This Article

Additional resources and features associated with this article are available within the HTML version:

- Supporting Information
- Links to the 31 articles that cite this article, as of the time of this article download
- Access to high resolution figures
- Links to articles and content related to this article
- Copyright permission to reproduce figures and/or text from this article

[View the Full Text HTML](#)

## Initial Observation of Magnetization Hysteresis and Quantum Tunneling in Mixed Manganese–Lanthanide Single-Molecule Magnets

Abhudaya Mishra,<sup>†</sup> Wolfgang Wernsdorfer,<sup>‡</sup> Khalil A. Abboud,<sup>†</sup> and George Christou<sup>\*†</sup>

Department of Chemistry, University of Florida, Gainesville, Florida 32611-7200, and  
Laboratoire Louis Néel-CNRS, 38042 Grenoble, Cedex 9, France

Received August 5, 2004; E-mail: christou@chem.ufl.edu

Single-molecule magnets (SMMs) are a growing class of materials that represents a molecular approach to nanoscale magnetic particles.<sup>1,2</sup> Such species derive their properties from the combination of a large ground-state spin ( $S$ ) and a large magneto-anisotropy of the Ising (easy-axis) type (i.e. a negative zero-field splitting (ZFS) parameter,  $D$ ). Since the initial discovery of the  $[\text{Mn}_{12}\text{O}_{12}(\text{O}_2\text{CR})_{16}(\text{H}_2\text{O})_4]$  family of SMMs,<sup>2</sup> a number of other structural types have been discovered, almost all of them being transition metal clusters, and the majority of them being Mn clusters containing at least some  $\text{Mn}^{\text{III}}$  ions. In contrast, the synthesis of heterometallic transition metal–lanthanide SMMs is an almost completely unexplored area. Indeed, there are only two 3d/4f complexes of this type, a  $\text{Cu}_2\text{Tb}_2$ <sup>3a</sup> and a  $\text{Dy}_6\text{Mn}_6$ .<sup>3b</sup> In general, the presence of a lanthanide ion's (i) large spin such as the  $S = 7/2$  of  $\text{Gd}^{3+}$  and/or (ii) large anisotropy as reflected in a large  $D$  value, could serve to generate SMMs with properties significantly different from those of homometallic transition metal SMMs. We have thus joined ongoing efforts in this area and have focused to date primarily on Mn-containing species. Note that we have in the past described a  $\text{CeMn}_8$  complex with  $S = 16$  that is an SMM,<sup>4</sup> but this contains diamagnetic  $\text{Ce}^{4+}$ , and therefore we do not consider it a mixed 3d/4f SMM but instead a “homometallic” Mn SMM. Note also that the previous 3d/4f SMMs<sup>3</sup> displayed frequency-dependent out-of-phase AC signals, but not reported were magnetization hysteresis loops or quantum tunneling behavior, two confirmatory properties of a SMM; we have therefore sought these properties in our 3d/4f complexes. In the present work, we report access to a new family of mixed  $\text{Mn}^{3+}$ – $\text{Ln}^{3+}$  polynuclear SMMs comprising a  $[\text{Mn}_{11}\text{Ln}_4]^{45+}$  core. Five isostructural clusters have been synthesized, and all but the Eu complex display frequency-dependent out-of-phase AC susceptibility signals suggestive of SMMs. Furthermore, we have confirmed that these complexes are SMMs by observing magnetization hysteresis loops and have also established that they exhibit quantum tunneling of the magnetization (QTM).

The reaction of  $[\text{Mn}_3\text{O}(\text{O}_2\text{CPh})_6(\text{py})_2(\text{H}_2\text{O})]$  (1 equiv) with  $\text{Ln}(\text{NO}_3)_3$  (2 equiv) ( $\text{Ln} = \text{Nd}, \text{Gd}, \text{Dy}, \text{Ho}, \text{and Eu}$ ) in  $\text{MeOH}/\text{MeCN}$  (1:20 v/v) gave a dark-brown solution, which was filtered and concentrated by evaporation to give dark crystals in 55–60% isolated yield of complexes all containing the  $[\text{Mn}_{11}\text{Ln}_4]^{45+}$  core, but differing slightly in the periphery. The Dy complex  $[\text{Mn}_{11}\text{Dy}_4\text{O}_8(\text{OH})_6(\text{OMe})_2(\text{O}_2\text{CPh})_{16}(\text{NO}_3)_5(\text{H}_2\text{O})_3] \cdot 15\text{MeCN}$  (**1**·15MeCN) will be discussed here. Complex **1** crystallizes<sup>5</sup> in the triclinic space group  $P\bar{1}$  and lies on an inversion center. The structure (Figure 1) consists of a  $[\text{Mn}_{11}\text{Ln}_4]^{45+}$  core held together by 2  $\mu_3\text{-O}^{2-}$ , 6  $\mu_4\text{-O}^{2-}$ , 6  $\mu_3\text{-OH}^-$  and 2  $\mu\text{-OMe}^-$  ions. Peripheral ligation is provided by 12  $\mu^-$  and 4  $\mu_3$ -benzoate groups, 5 chelating  $\text{NO}_3^-$  groups on the Dy ions, two  $\text{H}_2\text{O}$  molecules on Mn6 and Mn6a, and a water molecule on Dy2. The metal oxidation states ( $\text{Mn}^{3+}$  and  $\text{Dy}^{3+}$ ) and

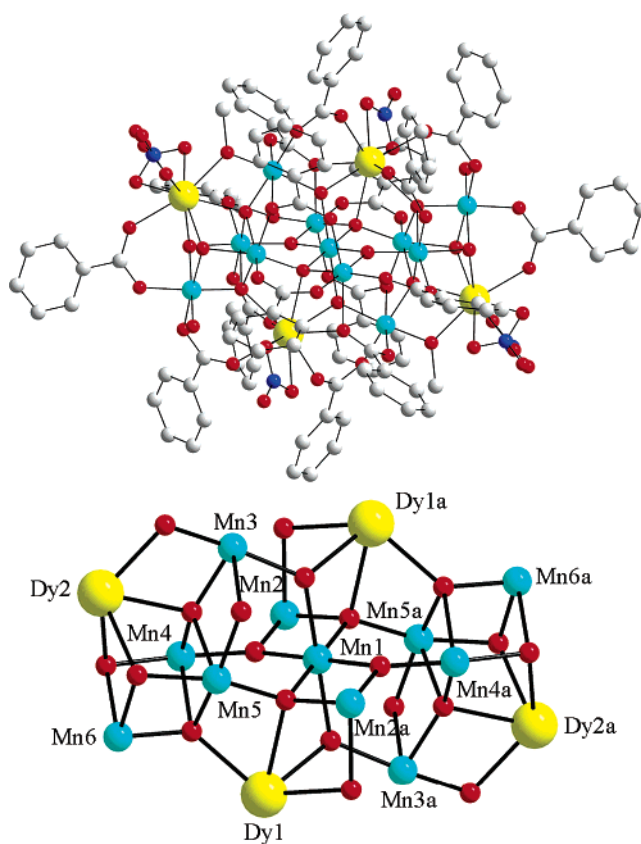


**Figure 1.** Molecular structure of **1** (top) and its centrosymmetric core (bottom). Color code: cyan, manganese; yellow, dysprosium; red, oxygen; blue, nitrogen; gray, carbon.

the protonation levels of  $\text{O}^{2-}$  and  $\text{OH}^-$  ions were established by bond valence sum calculations,<sup>6</sup> charge considerations, inspection of metric parameters, and the observation of  $\text{Mn}^{\text{III}}$  Jahn–Teller (JT) elongation axes. The Mn and Dy atoms are six- and nine-coordinate, respectively. Closer inspection of the core (Figure 1) reveals two distorted  $[\text{DyMn}_3\text{O}_4]$  cubanes, which are each linked by a Mn and Dy atom to a central linear  $\text{Mn}_3$  unit. The same core structure is found in the Nd, Gd, Ho, and Eu complexes.

Solid-state DC magnetic susceptibility ( $\chi_M$ ) data were collected in the 5.0–300 K range in a 1 kG (0.1 T) field. The  $\chi_M T$  value of  $74.3 \text{ cm}^3 \text{ mol}^{-1} \text{ K}$  at 300 K is less than the expected value for 11  $\text{Mn}^{3+}$  ( $S = 2$ ) and 4  $\text{Dy}^{3+}$  ( $S = 5/2, L = 5, {}^6\text{H}_{15/2}$ ) noninteracting ions of  $89.7 \text{ cm}^3 \text{ mol}^{-1} \text{ K}$ , consistent with antiferromagnetic exchange interactions, and decreases to  $57.1 \text{ cm}^3 \text{ mol}^{-1} \text{ K}$  at 5.0 K, suggesting that **1** has a large ground-state spin value. To investigate whether **1** might be a SMM, AC susceptibility measurements were carried out in a 3.5 G AC field oscillating at 10–1000 Hz, and with a zero DC field (Figure 2).

<sup>†</sup> University of Florida.

<sup>‡</sup> Laboratoire Louis Néel-CNRS.

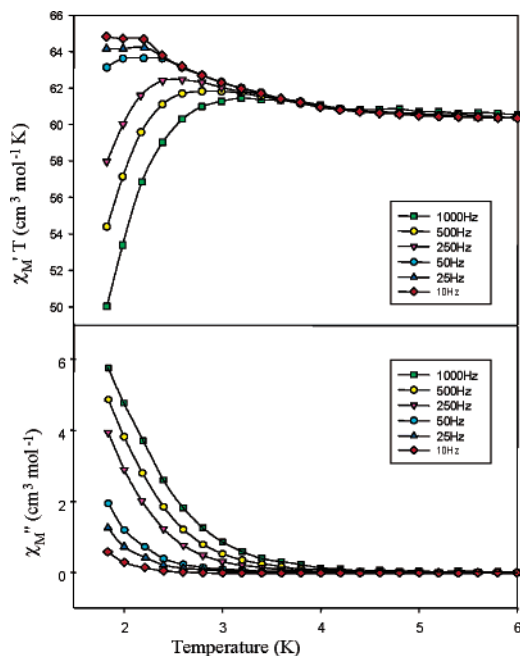


**Figure 2.** Plots of the in-phase ( $\chi_M'$ ) (top) and the out-of-phase ( $\chi_M''$ ) (bottom) AC susceptibility signals vs temperature for complex **1**.

A frequency-dependent decrease in the in-phase ( $\chi_M'$ ) signal and a concomitant increase in the out-of-phase ( $\chi_M''$ ) signal were observed, the latter merely “tails” of peaks that lie at  $<1.8$  K, the operating limit of our SQUID. These are indicative of slow magnetization ( $M$ ) relaxation. Such  $\chi_M''$  signals suggest the complex might be a SMM but do not prove it because intermolecular interactions and phonon bottlenecks can also give such signals.<sup>7</sup> Confirmation was therefore sought by magnetization vs DC field scans on single crystals of **1**·15MeCN using a micro-SQUID.<sup>8</sup> Magnetization hysteresis, the diagnostic property of a magnet, was indeed observed below  $\sim 1.0$  K (Figure 3, top). The observed loops show superparamagnet-like increasing coercivity with decreasing temperature, confirming **1** to be a SMM. No steps due to quantum tunneling of magnetization (QTM) were seen, probably due to a distribution of molecular environments and/or intermolecular interactions.<sup>9</sup> To characterize the system further, DC magnetization decay data were collected in the 0.04–1.0 K range: at each temperature, the magnetization was saturated with a DC field, the temperature lowered to a chosen value, the field switched off, and the magnetization monitored with time. This gave relaxation time ( $\tau$ ) vs  $T$  data, which were used to construct the Arrhenius plot of Figure 3 (bottom), based on the Arrhenius relationship  $\tau = \tau_0 \exp(U_{\text{eff}}/kT)$ . The slope in the thermally activated region above  $\sim 0.5$  K gave  $\tau_0 = 4 \times 10^{-8}$  s and  $U_{\text{eff}} = 9.3$  K. Below  $\sim 0.1$  K, the relaxation time becomes essentially temperature-independent, consistent with the purely quantum regime where QTM through the anisotropy barrier is only via the lowest energy  $\pm M_s$  levels.

Complex **1** is the first mixed-metal 3d/4f SMM to exhibit hysteresis loops and quantum tunneling of the magnetization. The ability to probe both classical (hysteresis) and quantum (QTM) magnetism behavior as a function of the lanthanide ion, as demonstrated by the extension of the synthetic method for **1** to several other lanthanides, should provide an invaluable means of improving our understanding of both the chemistry and physics of this area of bimetallic nanoscale magnetic materials. In addition, the large variation in spin and anisotropy within the lanthanide ions

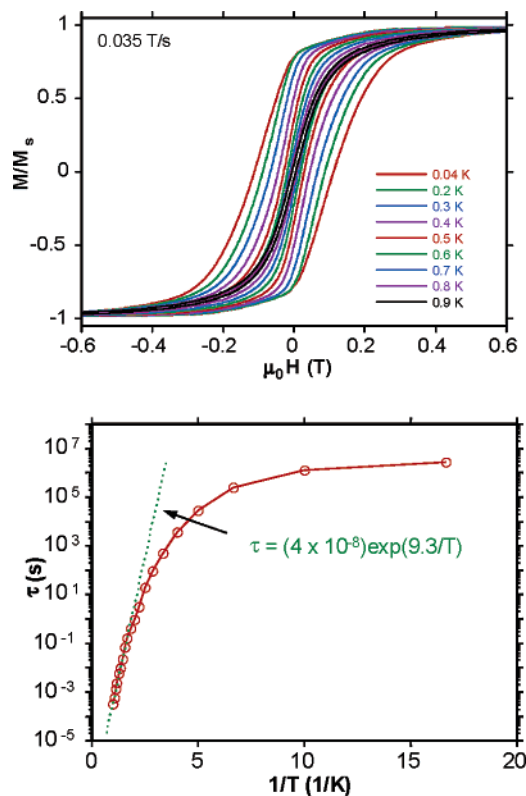


**Figure 3.** (Top) Magnetization ( $M$ ) vs field hysteresis loops for **1**·15MeCN at the indicated temperatures;  $M$  is normalized to its saturation value,  $M_s$ . (Bottom) Arrhenius plot constructed from DC magnetization decay data. The dashed line is the fit of the thermally activated region to the Arrhenius relationship with the indicated parameters.

mentioned earlier offers the enticing possibility of being able to raise the blocking temperature ( $T_B$ ) of SMMs to above that of the  $\text{Mn}_{12}$  family.

**Acknowledgment.** This work was supported by the National Science Foundation.

**Supporting Information Available:** Crystallographic details in CIF format. Bond valence sums and magnetism data. This material is available free of charge via the Internet at <http://pubs.acs.org>.

## References

- (1) Christou, G.; Gatteschi, D.; Hendrickson, D. N.; Sessoli, R. *MRS Bulletin* **2000**, 25, 66–71 and references therein.
- (2) (a) Sessoli, R.; Tsai, H. L.; Schake, A. R.; Wang, S.; Vincent, J. B.; Foltling, K.; Gatteschi, D.; Christou, G.; Hendrickson, D. N. *J. Am. Chem. Soc.* **1993**, 115, 1804–1816. (b) Sessoli, R.; Gatteschi, D.; Caneschi, A.; Novak, M. A. *Nature* **1993**, 365, 141–143.
- (3) (a) Osa, S.; Kido, T.; Matsumoto, N.; Re, N.; Pochaba, A.; Mrozinski, J. *J. Am. Chem. Soc.* **2004**, 126, 420–421. (b) Zaleski, C. M.; Depperman, E. C.; Kampf, J. W.; Kirk, M. L.; Pecoraro, V. L. *Angew. Chem., Int. Ed.* **2004**, 43, 3912–3914.
- (4) Tasiopoulos, A. J.; Wernsdorfer, W.; Moulton, B.; Zaworotko, M. J.; Christou, G. *J. Am. Chem. Soc.* **2003**, 125, 15274–15275.
- (5) (a) Anal. Calcd (Found) for dried **1** (solvent-free): C 35.75 (35.91), H 2.53 (2.56), N 1.83 (1.74). (b) Crystal data for **1**·15MeCN:  $\text{C}_{142}\text{H}_{139}\text{N}_{20}\text{O}_{66}\text{Mn}_{11}\text{Dy}_4$ , 4436.07 g mol<sup>-1</sup>, triclinic  $P1$ ,  $a = 16.5705(11)$  Å,  $b = 17.2926(11)$  Å,  $c = 18.6213(12)$  Å,  $\alpha = 64.9700(10)^\circ$ ,  $\beta = 67.2950(10)^\circ$ ,  $\gamma = 65.6110(10)^\circ$ ,  $Z = 1$ ,  $V = 4256.6(5)$  Å<sup>3</sup>,  $d_{\text{calc}} = 1.731$  g cm<sup>-3</sup>,  $T = 173$  K. Final  $R1 = 4.25$  and  $wR2 = 10.06\%$ .
- (6) (a) Bond valence sums for  $\text{Mn}^{\text{III}}$  and  $\text{Dy}^{\text{III}}$  ions of **1** were 2.88–2.92 and 2.89–2.90, respectively. (b) Liu, W.; Thorp, H. H. *Inorg. Chem.* **1993**, 32, 4102–4105. (c) Palenik, G. J. *Inorg. Chem.* **1997**, 36, 4888–4890.
- (7) Chakov, N. E.; Wernsdorfer, W.; Abboud, K. A.; Christou, G. *Inorg. Chem.* **2004**, 43, 5919–5930.
- (8) Wernsdorfer, W. *Adv. Chem. Phys.* **2001**, 118, 99–190.
- (9) Soler, M.; Wernsdorfer, W.; Foltling, K.; Pink, M.; Christou, G. *J. Am. Chem. Soc.* **2004**, 126, 2156–2165.

JA045272T